DIRECT MEASUREMENT OF THE TOTAL WIDTH OF THE η' MESON

E. Czerwiński[†*], P. Moskal[†*], D. Grzonka[*], A. Budzanowski[⋆],
R. Czyżykiewicz[†], D. Gil[†], M. Janusz[†*], L. Jarczyk[†], B. Kamys[†],
A. Khoukaz[‡], P. Klaja[†*], W. Oelert[*], C. Piskor-Ignatowicz[†], J. Przerwa[†*],
B. Rejdych[†], J. Ritman[*], T. Sefzick[*], M. Siemaszko[§], M. Silarski[†],
J. Smyrski[†], A. Täschner[‡], M. Wolke[*], P. Wüstner[*], M. Zieliński[†], W. Zipper[§]

[†] *Institute of Physics, Jagiellonian University, Cracow, Poland*
[*] *IKP & ZEL, Forschungszentrum Jülich, Germany*
[‡] *IKP, Westfälische Wilhelms-Universität, Münster, Germany*
[§] *Institute of Physics, University of Silesia, Katowice, Poland*
[⋆] *Institute of Nuclear Physics, 31-342 Cracow, Poland*

Abstract

Using stochastically cooled proton beam of the cooler synchrotron COSY and the COSY-11 apparatus we have measured the mass distribution of the η' meson producing it via the $pp \rightarrow pp\eta'$ reaction. The preliminary analysis shows that the achieved experimental mass resolution amounts to about 0.3 MeV (FWHM). Such precision with about 2300 events gathered at five excess energies should permit for the extraction of the width of the η' meson with an accuracy of about 10 keV. In this article we describe the method of the measurement and present preliminary results.

1 Introduction

Studies of the η' meson decays [1] and production [2] are of interest on its own and provide inputs to the phenomenology of the Quantum Chromo-Dynamics in the non-perturbative regime [3]. Specifically, precise determinations of the

partial widths for the η' decay channels should be helpful for the development of the Chiral Perturbation Theory. However, the experimental precision of the partial width for various decay channels – where only the branching ratio is known or will be measured – is governed by the precision of the knowledge of the total width. In the case of the η' meson the branching ratios are typically known with accuracy better than 1.5%, while the total width is established about 10 times less accurate [4]. Therefore, we expect that the precise determination of the natural width of the η' meson will have an impact on the physics results which will be derived from measurements at such facilities like e.g. COSY, DAϕNE-2 or MAMI-C carried out by collaborations: WASA-at-COSY [5], KLOE-2 [7,8] and CBall-at-MAMI [6] respectively.

In the last issue of the Review of Particle Physics only two direct measurements of the natural width of the η' meson are reported [4]. In the first experiment the width was established from the missing mass spectrum of the $\pi^- p \to nX$ reaction measured close to the threshold for the production of the η' meson [9]. The achieved experimental mass resolution was equal to 0.75 MeV/c^2 (FWHM) and the extracted value of $\Gamma_{\eta'}$ amounts to (0.28 ± 0.10) MeV/c^2. In the second experiment the value of $\Gamma_{\eta'} = (0.40 \pm 0.22)$ MeV/c^2 was derived from the threshold excitation function of the $pd \to {}^3He\,X$ reaction [10]. The mean value from the two direct measurements [9,10] amounts to (0.30 ± 0.09) MeV/c^2 [4] and differs strongly from the value of (0.202 ± 0.16) MeV/c^2 determined indirectly from the combinations of partial widths obtained from integrated cross sections and branching ratios [4].

During the many years of studies of the η' meson [11,12,13] by means of the stochastically cooled proton beam of COSY [14,15] and the COSY-11 apparatus (Fig. 1) we have achieved the accuracy of the mass determination comparable to the value of the natural width of the η' meson. This encouraged us to conduct the investigations of the $\Gamma_{\eta'}$ directly from the missing mass distribution of the $pp \to pp\eta'$ reaction measured near the kinematical threshold. The advantage of a study close to the threshold is that the uncertainties of the missing mass determination are considerably reduced since at threshold $\partial(mm)/\partial p$ tends to zero (mm = missing mass, p = momentum of the outgoing protons).

2　Experiment

The measurement of the $pp \to pp\eta'$ reaction was conducted for five discrete beam momenta: 3211, 3213, 3214, 3218, and 3224 MeV/c, where the threshold momentum is at 3208.3 MeV/c. It was carried out at the cooler synchrotron
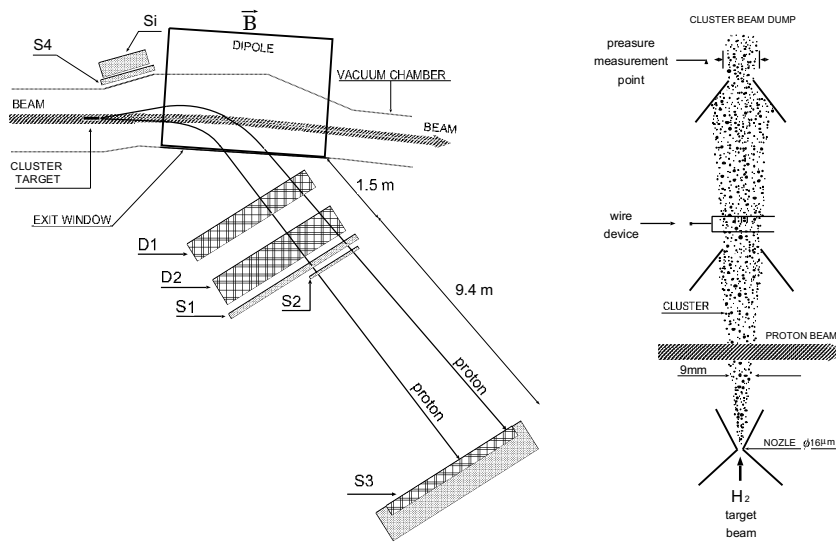
Figure 1: (left) COSY–11 detection setup with drift chambers (D1, D2) used for reconstruction of trajectories of positively charged ejectiles and scintillator hodoscopes (S1, S2, S3) for the time of flight determination. The silicon pad (Si) and scintillator (S4) detectors register the elastically scattered protons used for the monitoring purposes. (right) Schematic view of the target and beam crossing.

COSY [14, 15] using the COSY-11 facility [16, 17, 18]. At the intersection point of the cluster beam with the COSY proton beam the collisions of protons may result in the production of the η' meson. The ejected protons of the $pp \to pp\eta'$ reaction, having smaller momenta then the beam protons, are separated from the circulating beam by magnetic field, leave the vacuum chamber through a thin exit foil, and are registered by the detection system consisting of drift chambers and scintillation counters as depicted in Fig. 1 (left).

The measurement of the track direction by means of the drift chambers, and the knowledge of the dipole magnetic field and the target position allow to reconstruct the momentum vector for each registered particle. The time of flight measured between the S1 and the S3 scintillators gives the particle velocity. Independent determination of the momentum and velocity provides the particle identification. The knowledge of the momenta of both protons before and after the reaction allows to calculate the mass of a not observed particle or system of particles in the outgoing channel, which in case of the $pp \to pp\eta'$ reaction should be equal to the mass of the η' meson.
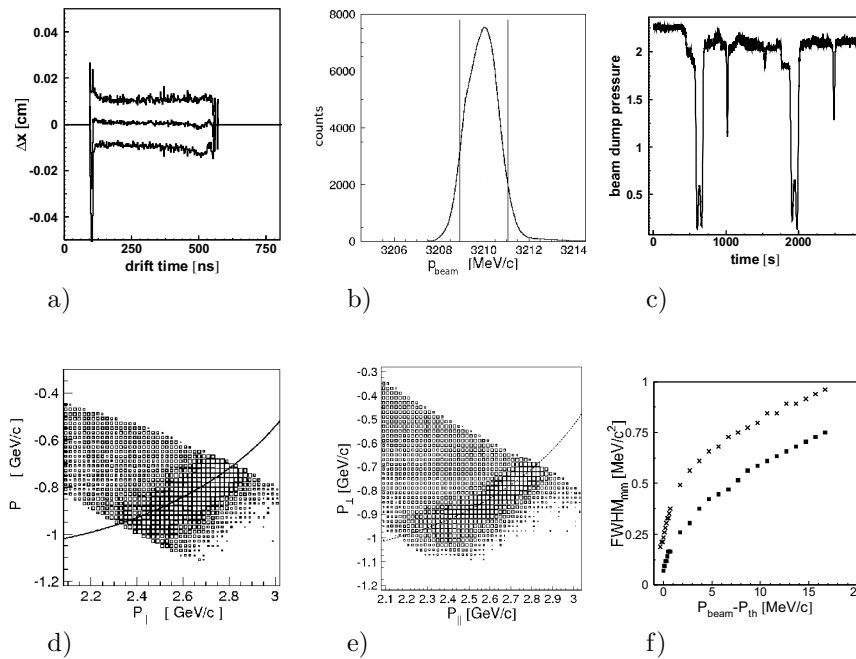
Figure 2: a) Average deviation (ΔX) between the measured and the fitted distances of tracks from the sense wire as a function of the drift time. The line around 0 corresponds to the average value of the ΔX distribution and the upper and lower lines denotes the spatial resolution ($\pm 1\sigma$) of the drift chamber. b) Beam momentum distribution obtained from the Schottky frequency spectrum measured during one of the previous COSY-11 runs. The range "seen" by 9 mm and 1 mm target is marked by the solid and dashed lines respectively. c) Distribution of the pressure measured during the wire device rotation. d,e) Momentum distribution of the forward scattered particles (in a logarithmic scale) with the superimposed kinematical ellipses (solid lines) expected for the elastically scattered protons. d) Data obtained with the target width of 9 mm and p_{beam} =2010 MeV/c [21]. e) On-line data from the reported here experiment conducted with the target width of circa 1 mm and p_{beam} =3211 MeV/c. f) FWHM of the missing mass signal as a function of beam momentum above the threshold for the η' meson creation in proton-proton collision simulated for 9 mm (crosses) and 1 mm (squares) target width [22].

In comparison to the previous measurement of the η' meson production, in order to improve the experimental resolution of the four-momentum determina-

tion and in order to decrease the spread of the momentum of the beam protons reacting with the target two major changes have been applied to the COSY-11 setup (Fig. 1). Namely, the spatial resolution of the drift chambers was improved by increasing the supply voltage up to the maximum allowed value and also the size of the target in the direction perpendicular to the COSY beam was decreased from 9 to circa 1 mm [19, 20].

2.1 Drift chambers

A charged particle passing through the drift cell ionizes gas molecules and the electrons drift towards the sense wire with a drift time related to the distance between the sense wire and the particle trajectory. The drift time to distance relation was calibrated for each 20 - 24 hours of the data taking period in order to minimize fluctuations of the drift velocity caused by variations of the atmospheric pressure, air humidity and gas mixture changes. Figure 2a illustrates that the obtained spatial resolution equals to about 100 μm.

2.2 Target

Due to the dispersion at the position of the COSY-11 target, the decrease in the target width results in a significant reduction of the momentum spread contributing to the measured events as shown in Fig. 2b. As can be clearly implied from the figure, the information about target size is crucial for determination of the beam momentum spread. It is also of great importance for the estimation of an error of momentum reconstruction of outgoing protons. Therefore, the spatial size of the target perpendicular to the COSY beam was controlled applying two independent methods. The first one is based on the movement of a wire through the cluster target beam which produces a pressure increase when a part of the cluster beam hits the wire. Several wires of different thicknesses on a rotating frame were used. The wire device was rotated several times through the cluster beam. The resulting pressure distribution as a function of rotation time is shown in Fig. 2c. Based on a preliminary analysis we expect to achieve an accuracy for the determination of the target size of about 0.2 mm.

The second technique used for monitoring the target beam size rest on the measurement of the momentum distribution of the elastically scattered protons (Fig. 2d,e). The momentum reconstruction of registered protons is performed by tracing back the trajectories from the drift chambers through the dipole magnetic field to the target centre. In reality, however, the reactions take place in a region of finite dimensions where beam and target overlap. Consequently, assuming in the analysis a point-like target implies a smearing of the momentum vectors. According to two–body kinematics, the momentum

components parallel and perpendicular to the beam axis form an ellipse. An example is shown in Fig. 2d,e. The spread around the expected kinematical ellipse can be used as a measure of the size of the interaction region [17]. For the appraisal of the effect in Fig. 2d,e we present results obtained with target widths of 9 and 1 millimetres.

2.3 Systematic uncertainty

The measurement of the missing mass distributions at five different beam energies will allow for monitoring the systematic uncertainties in the determination of the experimental mass resolution. This is mainly because the smearing of the missing mass due to the natural width of the η' remains unaltered when the beam momentum changes, whereas the smearing caused by the experimental uncertainties will narrow with decreasing beam momentum and at threshold it will reach a constant value directly proportional to the spread of the beam momentum. The effect is shown in Fig. 2f, which also illustrates that the reduction of the target thickness by 8 mm results in a change of the mass resolution by about 0.3 MeV. Since we expect to control the target thickness with an accuracy better then 0.2 mm, the systematical error due to the determination of the target size would be smaller than 0.01 MeV even if the measurement was conducted at only one excess energy.

Moreover, we can also distinguish the influence on the mass resolution caused by different experimental sources. For example angular distributions of the missing mass spectrum will permit to estimate contributions to the mass resolution due to the spread of the beam momentum and due to the proton momentum reconstruction [22]. This is because the resolution of the missing mass due to the spread of the beam momentum is almost independent of the polar emission angle of the η' meson, whereas the smearing of the missing mass due to the uncertainty of the proton momentum reconstruction does depend on this angle significantly [22].

3 Preliminary results

An on-line analysis has revealed a signal originating from the production of the η' meson at each of the investigated beam momenta (Fig. 3). As expected the width of the signal from the η' meson decreases with decreasing beam momentum, and closest to the threshold it equals to approximately 0.4 MeV (FWHM). Taking into account that the width of the η' is around 0.2 MeV we may estimate the achieved experimental resolution to be about 0.3 MeV, just at the same order as the searched signal. The presented spectra were obtained with a very preliminary calibration of the detection system. Hence,
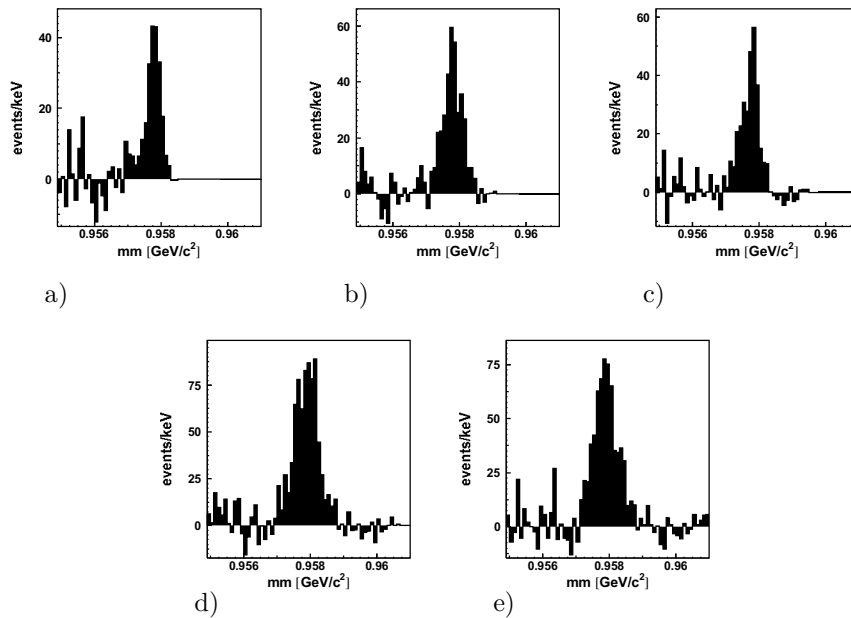
Figure 3: Preliminary background-corrected missing mass spectra for the $pp \rightarrow$ $pp\eta'$ reaction measured using the COSY–11 detection setup at the nominal beam momenta: a) 3211, b) 3213, c) 3214, d) 3218, e) 3224 MeV/c.

there is still a room for the improvement of the experimental resolution in the ongoing off-line analysis. In addition, independently of the improvement of the calibrations we will correct also for the effect of the possible broadening due to the changes of the beam optics which could cause variations of the beam momentum in the order of 10^{-5}. In order to enable such corrections we have monitored various parameters which could influence the beam conditions like current intensity in the COSY dipoles, the temperature of the cooling water of the magnets, air temperature, humidity, and barometric pressure inside the COSY tunnel. Independently, it will be possible to correct the variation of the beam momentum based on the distribution of the elastically scattered protons measured simultaneously with the $pp \rightarrow pp\eta'$ reaction.

4   Acknowledgements

References

1. A. Kupść, AIP Conf. Proc. **950**, 165 (2007).

2. P. Moskal, e-Print: hep-ph/0408162 (2004).

3. B. Borasoy and R. Nißler, AIP Conf. Proc. **950**, 180 (2007).

4. W.-M. Yao *et al.* (Particle Data Group), J. Phys. G **33**, 1 (2006).

5. H.-H. Adam *et al.*, e-Print Archive: nucl-ex/0411038 (2004).

6. A. Thomas, AIP Conf. Proc. **950**, 198 (2007).

7. F. Ambrosino *et al.*, Eur. Phys. J. **C50**, 729 (2007).

8. C. Bloise, AIP Conf. Proc. **950**, 192 (2007).

9. D. M. Binnie *et al.*, Phys. Lett. B **83**, 141 (1979).

10. R. Wurzinger *et al.*, Phys. Lett. B **374**, 283 (1996).

11. P. Moskal et al., Phys. Rev. Lett. **80**, 3202 (1998);

12. P. Moskal et al., Phys. Lett. **B 474**, 416 (2000);

13. A. Khoukaz et al., Eur. Phys. J **A 20**, 345 (2004);

14. D. Prasuhn *et al.*, Nucl. Instr. & Meth. A **441** 167 (2000).

15. H. Stockhorst *et al.*, AIP Conf. Proc. **950**, 239 (2007).

16. S. Brauksiepe *et al.*, Nucl. Instr. & Meth. A **376**, 397 (1996).

17. P. Moskal *et al.*, Nucl. Instr. & Meth. A **466**, 448 (2001).

18. J. Smyrski *et al.*, Nucl. Instr. & Meth. A **541**, 574 (2005).

19. H. Dombrowski *et al.*, Nucl. Instrum. Meth. A **386**, 228 (1997).

20. A. Täschner *et al.*, AIP Conf. Proc. **950**, 85 (2007).

21. R. Czyżykiewicz, e-Print: nucl-ex/0702010; PhD thesis, Jagiellonian University (2007).

22. E. Czerwiński, Diploma thesis, Jagiellonian University (2006).